RESEARCH ARTICLE

# Modeling and simulation of a conical dielectric probe instrument for skin cancer detection applications

Elnaz Poorreza[1], Noushin Dadashzadeh Gargari*[2]

[1] Ph. D, Faculty of Electrical engineering, Sahand University of Technology, Tabriz, Iran
2* Department of Electrical Engineering, Aras Branch, Islamic Azad University, Jolfa, Iran

**ARTICLE INFO**

***Article History:***

*Received 2024-10-09*
*Accepted 2024-12-09*
*Published 2024-02-15*

***Keywords:***

*Heat transfer,*
*Temperature distribution,*
*Temperature change,*
*Skin cancer,*
*Conical dielectric probe,*
*Microwave.*

**ABSTRACT**

Conventional techniques for diagnosing skin cancer include shape, size and skin tumor color, bleeding, a disorder in the tumor, and so on. The goal of researchers in this field of study is to find simpler and safer methods for cancer tumor detection. The conical dielectric probe will be an effective instrument for analyzing mankind tissue illnesses like the initial stage of skin cancer. This illness will be incredibly treatable when the tumors are distinguished at the initial stages. The possibility of making a probe to detect the cancerous cells with the least destructive side effect in the early stages was evaluated. Our research examined the input applied frequency variations (35GHz, 45GHz, 65GHz, and 90GHz) according to the microwave-based detection method and compared the obtained results, which are required for a better understanding of heat transfer and necrotic properties in the biological objects. According to the microwave reflection characteristics, developed models and simulations based on the finite element method, by increasing the frequency, the temperature change increases, and the proportion of damaged tissue increases slightly after 10 minutes of millimeter wave exposure.

**How to cite this article**
*Poorreza E., Dadashzadeh Gargari N., Modeling and simulation of a conical dielectric probe instrument for skin cancer detection applications. J. Nanoanalysis., 2024; 11(1): 636-645.*

## INTRODUCTION

The skin as the outermost layer of the human body acts as the initial barrier against pathogens, chemicals, mechanical damage, and UV light. In addition to its function as a protective obstacle, the skin supports people keep the right internal temperature and allows them to sense the world through nerve endings. The skin as a complex organ, is not a homogenous structure but consists of a number of different layers with different anatomy and function.

*Corresponding Author Email: *noushindadashzadeh@yahoo.com*

The three main layers of the skin are the epidermis, dermis, and hypodermis that are divided into several sub-layers. Giving the skin its color and protecting the body from the external environment are the responsibilities of the epidermis layer. The water content is the lowest in the stratum corneum, which is the outermost layer of the skin and part of the epidermis, and hydration increases toward the inner layers [1-4].

Skin cancers are cancer types that result from the skin tissue where other vital organs are protected by this outer layer of the body. They are due to the development and spreading of abnormal cells that have the ability to invade or spread to other parts of the body to make problems in their performance. It can be classified into two categories: melanoma and non-melanoma types. Melanoma is an aggressive skin cancer type because it can spread and invade other organs rapidly [5-9]. The current diagnostic procedure to detect skin cancer is based on a visual analysis involving full-body examination by a qualified physician using dermatoscopy. However, naked-eye observations have drawbacks such as low accuracy and false detections therefore it is regarded as a handicap in the detection process.

Microwaves which are electromagnetic waves with high frequency, have been successfully applied to a wide range of applications, such as dielectric materials evaluations and medical diagnostic and therapy areas [10, 11]. Microwave therapy system is preferred to surgery for most cancer types because it is a non-invasive process [12]. It is one of the standard treatment methods with fewer treatment-related side effects, therefore it is preferred to other methods [13].

Microwave-based detection method has gained increasing attention for early detection and diagnosis of cancer cells before they develop in other organs [14-17]. Electromagnetic measurement has been applied to biological tissue and the discovered difference in dielectric properties between healthy normal tissue and malignant tumor tissue raised the hopes toward the application of microwave for medical diagnostics, especially in cancer tumor detection fields.

Microwave measurement techniques on the skin have been used by numerous researchers for different applications, including the plain determination of the skin permittivity, the evaluation of skin tissue hydration for cosmetic investigation, and the monitoring of wound healing in medicine. Microwave reflectometry with open-ended coaxial probes or rectangular microwave probes has so far been the most commonly used method. Data for the permittivity of skin and skin tumors indicates that there is sufficient contrast between cancer and healthy skin tissue in the microwave band [1]. This contrast is a key factor for determining the healthy cell from the cancerous cell by this type of detection.

In designing a diagnostic system, the spatial resolution, frequency range and depth of sense are the factors that play important role. For those sensors that target the diagnosis or detection of skin cancer cells, a sensing depth in the range of several hundred micrometers up to one millimeter and sub-millimeter spatial resolution is sufficient [1].

Good coupling of the microwave high-frequency signal into biological organs is an important factor for high-sensitivity measurements and diagnostics. When designing a microwave system for medical purposes, there are several aspects that must be considered for better performance of the system [18].

The dielectric properties of skin tissue are directly related to parameters such as water, sodium, and protein content, which varies prominently between normal skin and malignant tumors. The water content for normal skin is around 60.9% and that for the malignant tumors is 81.7% [19]. These variations in

water content are detectable in the microwave measurements range. Malignant tissue also has higher sodium content than normal skin, therefore it causes more absorption of water and takes on higher values of permittivity and conductivity. The differences in protein content of normal and up-normal tissue, may result in variations in the relaxation frequency that contributes to differentiation among these tissues in microwave measurements [19]. At microwave frequency ranges, the dielectric properties of normal skin can be distinguished from those of cancer tumors by measuring their reflection properties in early-stage of the tumor. The reflection properties of tissues that are measured by microwave measurement techniques, are directly affected by the dielectric properties of the different materials [19, 20].

In order to optimize the dielectric conical probe design with respect to measurement contrast, a good understanding of the microwave interaction with skin is needed. Several factors are important for use in clinical practical applications. However, before real experimental cancer therapy, there should be basic numerical modeling and simulation. As a result, the modeling of a conical probe is needed for a better and more profound understanding of wave propagation, heat transfer mechanism and the fraction of necrotic tissue.

To date, very few studies have been reported on the simulation of the dielectric conical probe for a skin cancer diagnosis. It motivated us to perform a series of simulations by the finite element method to better realize the probe performance. It is generally a good idea to be aware of how the variation of applied microwave frequency affects the profiles such as the temperature distribution around the tissue which is related to the heat transfer mechanism, the necrotic fraction of tissue and so on.

In this work, the electromagnetic and bio-heat equations are coupled together. Since the working frequency has a great effect on several aspects of the detection, with regard to its special characteristics, the operating frequency of the probe is varied between 35GHz, 45GHz, 65GHz and 90GHz. In the following numerical research, some input data for the microwave conditions, with different frequencies and the contrast between variable frequencies of 35GHz, 45GHz, 65GHz and 90GHz and corresponding results are presented.

## MODEL DEFINITION

*Parameters, geometry and boundary conditions*

The millimeter waves of two microwave frequencies of 35 GHz and 95 GHz are regarded to be very sensitive to the materials with high water content. In this work, the utilization of a low-power 35 GHz, 45GHz, 65GHz, and 90GHz Ka-band millimeter wave and their reflectivity to moisture for non-invasive tumor detection has been carried out. Because skin tumors contain more moisture content in comparison with healthy ones, it results in stronger reflections profiles on this frequency range.

The abnormalities detections by the probe are defined in terms of S-parameters at the locations in which tumor cells exist. By using a 2D axis symmetric simulation model, microwave transition by a circular waveguide and a conically tapered dielectric probe to the target zone, is performed by the finite element method. The temperature changes of the skin tissue and the rate of damaged tissue analysis are conducted in the following section. According to Figure 1, the simulated model containing a circular waveguide, a tapered PTFE dielectric probe, and a phantom, regarding skin chunks. The entire presented model is bounded by an air domain regarding its outermost shell with perfectly matched layers (PML) boundary conditions to be capable of absorbing any radiation from the rod or reflected radiation from the skin phantom area. One terminal of the waveguide terminates with a circular port and is actuated utilizing the dominant $TE_{1m}$ mode.

Here m denotes the azimuthal mode number of this presented 2D axisymmetric model which is regarded as 1 in the Electromagnetic Waves, Frequency Domain physics interface settings. The other terminal of the waveguide is adjoined to a tapered conical PTFE dielectric ($\varepsilon_r$ =2.1) rod. As demonstrated in the figure, the shape of the rod is symmetrical. Therefore, its radius increases from the inside to the outside of the waveguide, therefore for impedance matching purposes, between the two domains of a waveguide and the air, it decreases gradually. The ring-shaped structure in the middle part, makes the rod connected and stabilized on the edge of the waveguide. The ending point of the tapered rod touches the skin phantom and is in direct contact with the skin tissue.

For neglecting any dissipation of the system, the conductivity of the metallic waveguide is regarded to be high value and is modeled as a perfect electric conductor (PEC). With the chosen radius of the proposed waveguide and the applied TE mode to the system, the cut-off frequency is near 29.3 GHz, which is determined by the following equation:

$$f_{cml} = \frac{C_0 P'_{nm}}{2\pi a} \quad (1)$$

$C_0$ shows the speed of light, $p'_{nm}$ denotes the root derivatives of the Bessel functions $J_n(x)$, $m$ and $n$ shows the mode indices, and $a$ shows the waveguide radius. The value of $p'_{11}$ is considered approximately 1.841. The operating frequencies of the probe, 35 GHz, 45GHz, 65GHz and 90GHz are higher than the waveguide cut-off frequency. The applied microwave is propagating through the waveguide.

As shown in Figure 2, the circular port boundary condition is considered on the inner boundary where the reflection and transmission characteristics of the applied microwave are calculated according to S parameters. In the setting section of the port boundary condition, PEC backing is regarded in the slit boundary condition part. The input power is considered about 1[mw].

Table 1 shows the geometry and operating conditions of the designed dielectric conical probe. As shown in Table 2, the electromagnetic properties of the designed model, are analyzed without a phantom. The complexity, for a healthy phantom then for a phantom containing a skin tumor is added in the next step.

Because the waveguide actuation occurs by low input power, it is expected harmless in this condition. Its influence on necrotic tissue is studied by analyzing Bioheat Transfer as well as temperature, in a 10-minute scale-time.

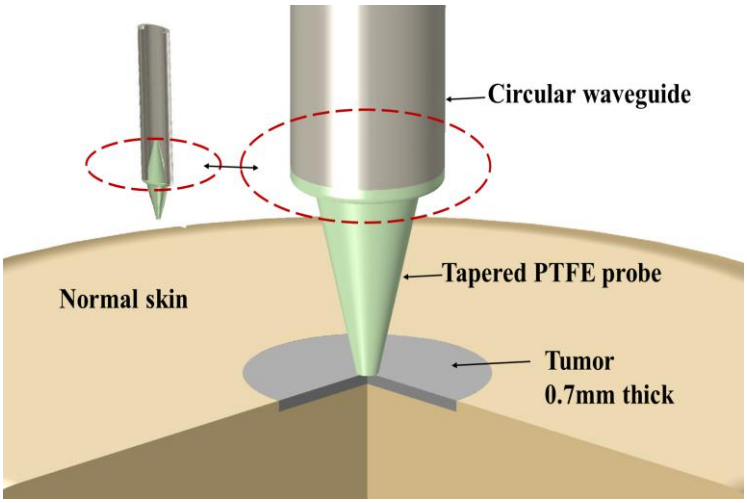


**Fig. 1.** The zoomed 3D picture of the skin tumor area. The entire dielectric probe model is simulated in a 2D axis symmetric dimension. The calculated S-parameters vary according to the different moisture content in each skin phantom.

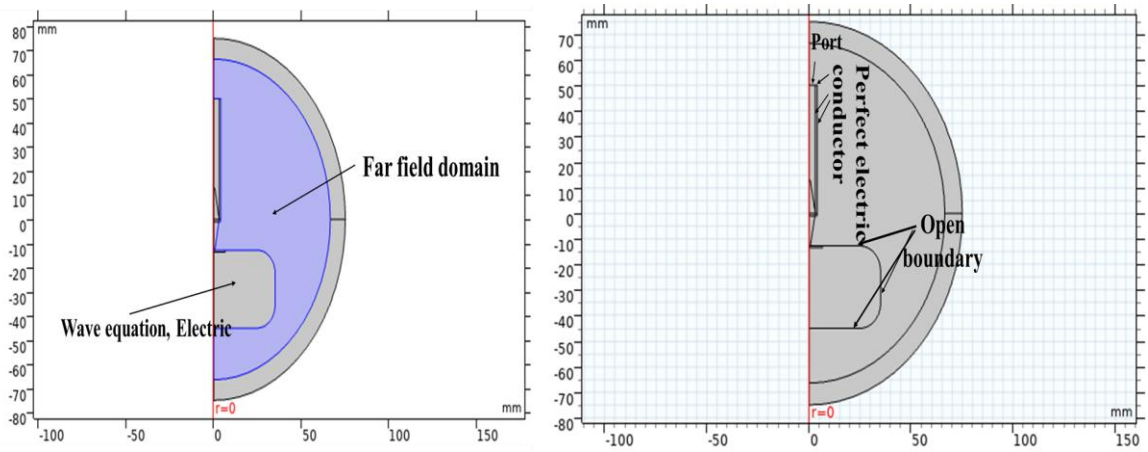


**Fig. 2.** Boundary conditions of conical probe.

**Table 1.** Operating conditions.

| Name | Expression | Value | Description |
|---|---|---|---|
| $f_c$ | 1.841*c_const/2/pi/r1 | 2.928E10 1/s | Cut-off frequency |
| $f_0$ | 35[GHz],45[GHz], 65[GHz], 90[GHz] | 9E10 Hz | Frequency |
| $r_1$ | 0.003[m] | 0.003 m | Waveguide radius |
| lda0 | c_const/f0 | 0.003331 m | Wavelength, free space |
| l_probe | 12.8[mm] | 0.0128 m | Tapered probe length |
| $w_1$_probe | 3[mm] | 0.003 m | Tapered probe width1 |
| $w_2$_probe | 0.58[mm] | 5.8E-4 m | Tapered probe width2 |
| $T_0$ | 34[degC] | 307.15 K | Initial skin temperature |

**Table 2.** Material property of the set-up.

| Property | Probe only | healthy phantom | tumor |
|---|---|---|---|
| Relative permittivity (imaginary part) | 0 | 10 | 15 |
| Relative permittivity (real part) | 1 | 5 | 8 |

## BIOLOGICAL HEAT EXCHANGE

Pennes' bio-heat equation, has been widely applied to solve the biological heat transfer. This equation describes how heat transfer happens inside biological tissue. This equation can be defined as follows [12]:

$$\rho C \frac{\partial T}{\partial t} = \nabla \cdot (k_{th} \nabla T) + \rho_b C_b \omega_b (T_b - T) + Q_{met} + Q_{ext} \quad (2)$$

here, the left side of Eq. (2) indicates the transient term. The first, second, third and fourth terms on the right side, indicate conduction of heat, heat loss by the blood flow, internal heat or metabolic heat

source, and external heat source (heat which is created by the applied electric field), respectively. ($\rho_b$ is the blood density, $C_b$ is the specific heat capacity of the blood, $\omega_b$ is the blood perfusion rate, $T_b$ is the arterial blood temperature, and $K_{th}$ is the thermal conductivity). The external heat source takes into account the effects of the resistive heat formed by the electromagnetic field which can be defined as [12]:

$$Q_{ext} = \frac{1}{2}\sigma_{Liver}\left|\vec{E}\right|^2 \quad (3)$$

The temperature rise is affected by electrical properties. When microwave waves propagate, their energy is absorbed by the tissue and converted into internal heat generation, raising the temperature of the tissue. In our study, since the probe is outside of the skin tissue, the second and third term in Eq. (2) is zero ($C_b$, $\omega_b$ and $\rho_b$ are zero). $T_b$ is considered 310.15[K].

**SIMULATION RESULTS**:

Figure 3 shows the real part of the electric field $E_r$ excited from one end of the waveguide with a tumor phantom. As the figure shows, by increasing the Frequency from 35GHz to 90GHz, the density of wave fronts increases. The maximum electric field with red color, varies between 150 to 300 (V/m). When the tissue is not considered, the entire field passes and at the end of the conical probe it gradually diverges. But when the tissue is considered, the reflection of electromagnetic waves is observed. This field is in the form of spherical wave fronts and is stronger near the tip of the waveguide.

is the temperature parameter. In other words, this model is based on the temperature difference between the environment and the surface of the tissue (k (T0-T). Because the temperature of tissue which contains a tumor is higher than the temperature of tissue without a tumor, this temperature change is a good help to the diagnosis and the location of the tumor.

Temperature change on the surface of the phantom with the tumor area is depicted in Figure 4. Since the low input power of the waveguide port is considered around 1 mW, the temperature change is within 0.05 °C even after 10 minutes of millimeter wave exposure. These temperature variations with tumor cells are larger than in the case without tumor cells. It helps to diagnose the tumor cells from healthy ones. As the frequency increases from 35GHz to 90GHz, the temperature increases and reaches 0.3 °C. The color difference indicates the relatively hotter spot where the temperature is still very close to the initial temperature of 34 °C. It is easily expected that the temperature variation is less than the case with the tumor because the resistive loss should be lower due to the smaller imaginary part of the permittivity of the healthy skin.

According to Figure 5, the damaged tissue ratio is presented. It shows that the influence of the low-power millimeter wave can be neglected. As shown in the figure, the level of necrotic tissue is extremely low even after 10 minutes of microwave exposure. In spite of the fact that the maximum rate of tissue necrosis value increases with increasing frequency from 35GHz to 90 GHz, it is not significant in all cases. It can be seen that by increasing the input frequency, the area of necrosis becomes smaller and does not cover the entire area. Figure 6 shows the resistive losses in the case where the tumor is added in the middle of the center the top of skin surface. The value of resistive losses induced by the temperature, increases with increasing the applied microwave frequency.

The calculated S-parameters show more reflection when the skin with the tumor is considered, according to its higher moisture ingredient, and they are summarized as shown in Table 3.

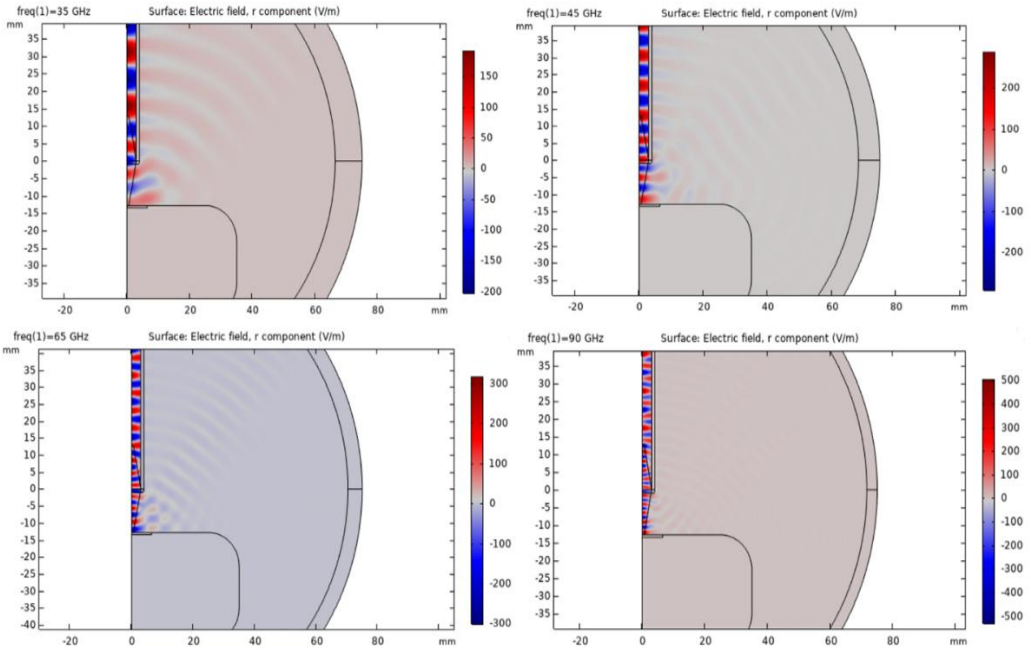


**Fig. 3.** Wave propagation from the dielectric rod depicted with the $E_r$ component of the E-field.

One of the most important parameters which play a key role in determining and diagnosing skin cancer

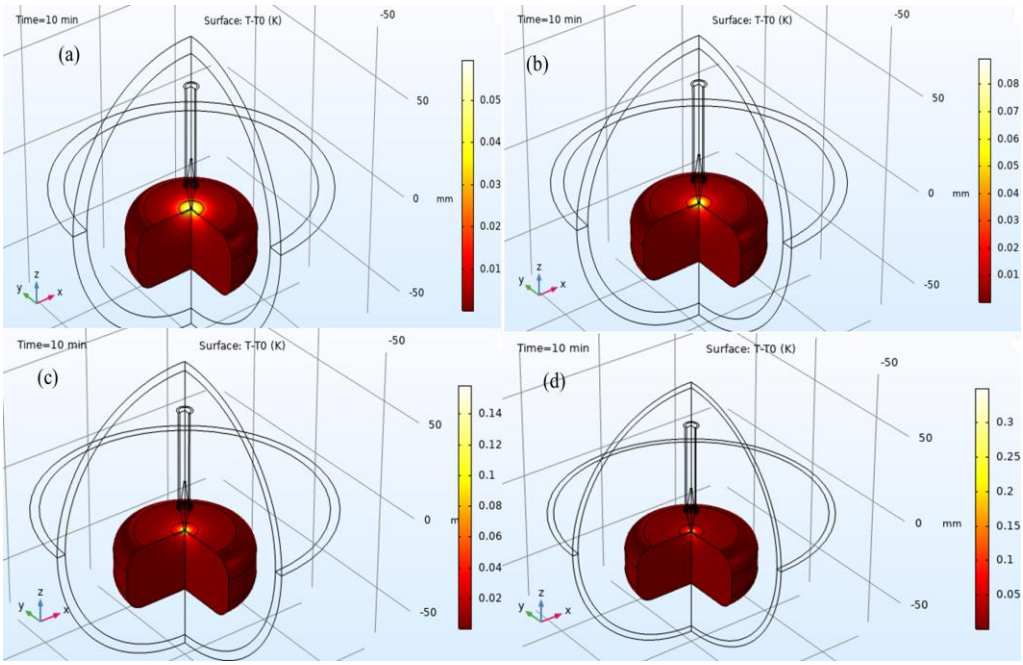


**Fig. 4.** The temperature profiles after 10 minutes, when the microwave frequency varied from 35[GHz],45[GHz], 65[GHz], 90[GHz].

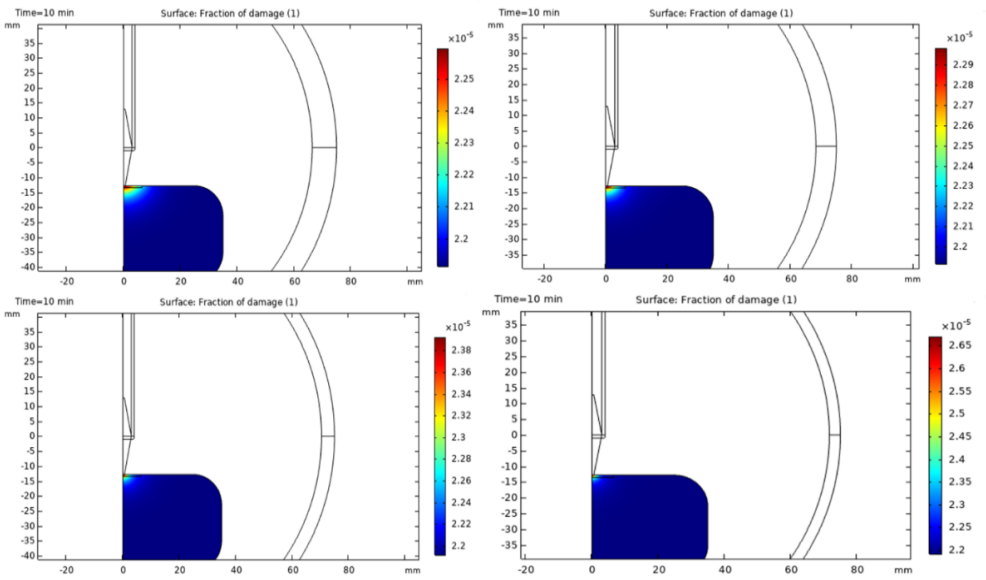


**Fig. 5.** The level of necrotic tissue after 10 minutes of millimeter wave exposure when the microwave frequency varied from 35[GHz],45[GHz], 65[GHz], 90[GHz].

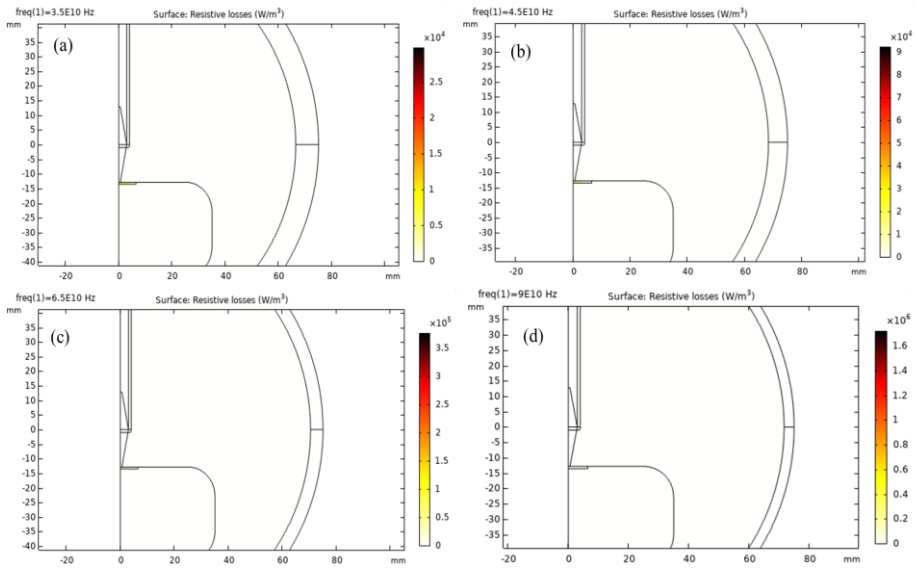


**Fig. 6.** The resistive losses in the case when the microwave frequency varied from 35[GHz],45[GHz], 65[GHz], 90[GHz].

**Table 3.** S-Parameter response of the conical probe

| | Probe only | With normal Phantom | Tumor added |
|---|---|---|---|
| S11 | -29.5 dB | -9.84 dB | -8.97dB |

The electromagnetic material properties of skin and tumor at 35 GHz are approximated to show the feasibility of the S-parameter method by detecting the areas with higher moisture content. Figure 7 shows the graphical representations of far-field patterns in the frequency range of 35, 45, 65 and 90 GHz. As it can be

seen, the radiation is from the tapered probe toward the top side. From these presented patterns, the location of cancerous tumors can be determined.

In the following section of our work, temperature change of skin tissue at the presence of tumor, at the frequency of 35GHz in times of 0, 1, 3, 5, 8, and 10 minutes were carried out. Figure 8 shows the 3D representation of the growth rate of tissue temperature with time at 0, 1, 3, 5, 8, and 10 minutes at frequency of 35GHz. As it can be clearly seen with the increase of time the amount of temperature increases and it covers the entire tumor area.

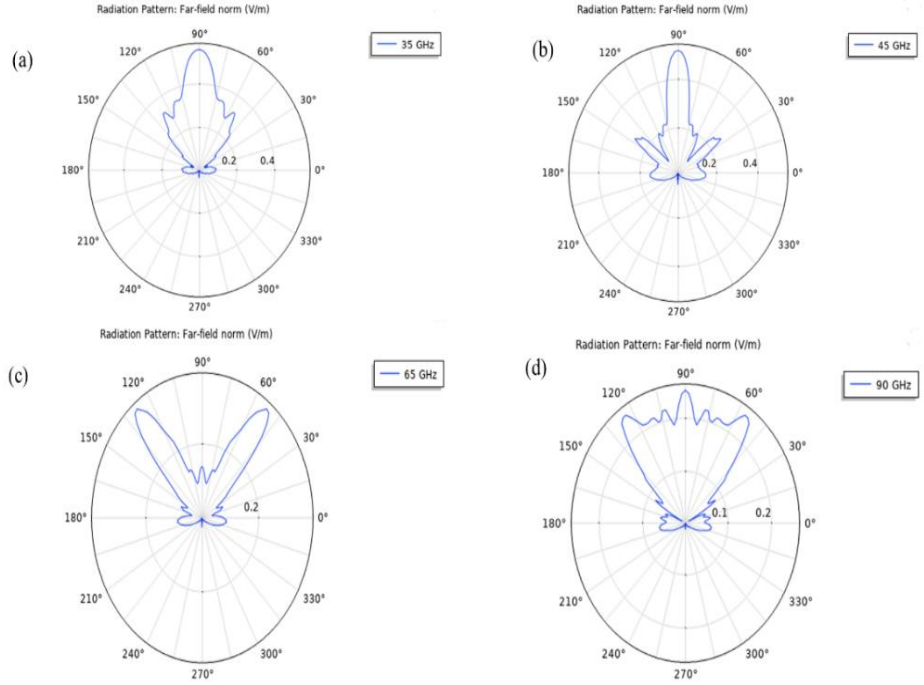


**Fig. 7.** The Far-field patterns in the frequency range of 35, 45, 65 and 90 GHz indicate the radiation from the tapered probe toward the top side.

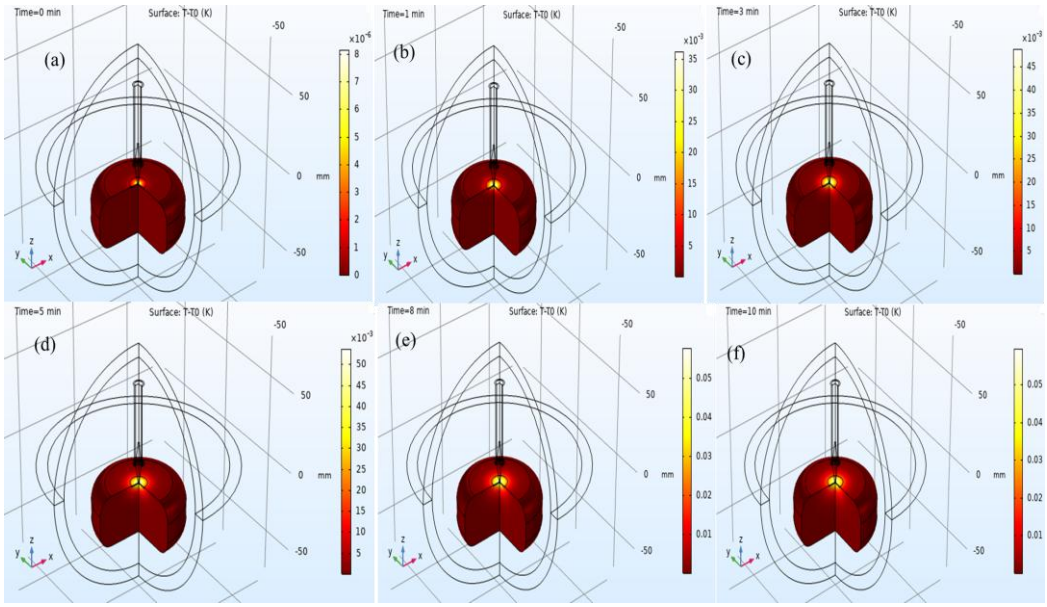


**Fig. 8.** The pattern of changes in temperature around the phantom in the presence of a tumor between 0 and 10 (0, 1, 3, 5, 8 and 10 minutes) minutes at 35 GHz.

## CONCLUSION

The contribution of water content is important since normal skin and cancerous lesions differ in their water content as well as their salinity. Microwave signals are sensitive to both of these parameters, making these measurements ideal for skin cancer detection purposes. The results of this presented study indicate that using dielectric conical probes to measure the variation of skin properties holds promise for skin cancer tumor detection. Our work examined the input frequency variations applied and compared the obtained results, which are required for a better understanding of the heat change and necrotic properties. According to the microwave reflection characteristics, developed models and simulations, by increasing the frequency, the temperature change increases and the proportion of damaged tissue increases (not significantly) after 10 minutes of millimeter wave exposure.

## REFERENCES


1. F. Töpfer and J. Oberhammer, in *Principles and Applications of RF/Microwave in Healthcare and Biosensing*, Elsevier, 2017, pp. 103.
2. F. Töpfer, S. Dudorov and J. Oberhammer, 2012.
3. M. K. Sharma, R. Kumari, A. Mittal, M. K. Upadhyay, A. Mittal and K. Singh, in *Flexible Electronics for Electric Vehicles*, Springer, 2023, pp. 47.
4. S. T. Sucharitha, I. Kannan and K. Varun Kumar, in *Intelligent Computing and Applications*, Springer, 2023, pp. 281.
5. S. Mumtaz, J. N. Rana, E. H. Choi and I. Han, Int. J. Mol. Sci., 2022, vol. 23, no. 16, 9288.
6. J. Boparai and M. Popović, *Sensors*, 2022, vol. 22, no. 5, pp. 1955.
7. E. V. Salomatina, B. Jiang, J. Novak and A. N. Yaroslavsky, *J Biomed Opt,* 2006, vol. 11, no. 6, pp. 064026.
8. V. Andreeva, E. Aksamentova, A. Muhachev, A. Solovey, I. Litvinov, A. Gusarov, N. N. Shevtsova, D. Kushkin and K. Litvinova, *Diagnostics*, 2022, vol. 12, no. 1, pp. 72.
9. H. Lui, J. Zhao, D. McLean and H. Zeng, *Cancer research*, 2012, vol. 72, no. 10, pp. 2491.
10. A. K. Gupta, P. K. Rao and R. Mishra, in *VLSI, Microwave and Wireless Technologies*, Springer, 2023, pp. p. 625.
11. M. Selmi, A. A. Bin Dukhyil and H. Belmabrouk, *Appl. Sci.*, 2019, vol. 10, no. 1, p. 211.
12. P. Keangin, P. Rattanadecho and T. Wessapan, *Int. Commun. Heat Mass Transf.*, 2011, vol. 38, no. 6, pp. 757.
13. P. Keangin and P. Rattanadecho, *Adv. Mech. Eng.*, 2018, vol. 10, no. 8, p. 1687814017734133.
14. P. Rattanadecho and P. Keangin, *Int. Commun. Heat Mass Transf.*, 2013, vol. 58, no. 1-2, pp. 457.
15. X. Wu, B. Liu and B. Xu, *Appl. Therm. Eng.*, 2016, vol. 107, pp. 501.
16. S. Kabiri and F. Rezaei, *Scientific Reports*, 2022, vol. 12, no.1, pp. 1.
17. A. Kabiri and M. R. Talaee, *Heat Mass Transf*, 2019, vol. 55, no. 8, pp. 2199.
18. G. Deshazer, P. Prakash, D. Merck and D. Haemmerich, *Int J Hyperthermia*2017, vol. 33, no. 1, pp. 74.
19. P. Mehta, K. Chand, D. Narayanswamy, D. G. Beetner, R. Zoughi and W. V. Stoecker, *IEEE Trans Instrum Meas*, 2006, vol. 55, no. 4, pp. 1309.
20. M. Gniadecka, P. A. Philipsen, S. Wessel, R. Gniadecki, H. C. Wulf, S. Sigurdsson, O. F. Nielsen, D. H. Christensen, J. Hercogova and K. Rossen, *J. Invest. Dermatol.*, 2004, vol. 122, no. 2, pp. 443.